

Electrospun polyethersulfone affinity membrane: Membrane preparation and performance evaluation

Zuwei Ma^{a,*}, Zhengwei Lan^a, Takeshi Matsuura^b, Seeram Ramakrishna^a

^a Nanoscience and Nanotechnology Initiative, National University of Singapore, 9 Engineering Drive 1, Singapore 117576, Singapore

^b Department of Chemical Engineering, University of Ottawa, 161 Louis Pasteur, Ottawa, Ont. K1N 6N5, Canada

ARTICLE INFO

Article history:

Received 9 July 2009

Accepted 12 September 2009

Available online 17 September 2009

Keywords:

Affinity membrane
Frontal analysis
Breakthrough
Electrospinning
Polyethersulphone (PES)
IgG purification
Spin column
Protein A/G
Plate model

ABSTRACT

Non-woven polyethersulfone (PES) membranes were prepared by electrospinning. After heat treatment and surface activation, the membranes were covalently functionalized with ligands to be used as affinity membranes. The membranes were characterized in terms of fiber diameter, porosity, specific area, pore size, ligand density and binding capacities. To evaluate the binding efficiency of the membrane, dynamic adsorption of bovine serum albumin (BSA) on the Cibacron blue F3GA (CB) functionalized PES membrane was studied. Experimental breakthrough curves were fitted with the theoretical curves based on the plate model to estimate plate height (H_p) of the affinity membrane. The high value of H_p (1.6–8 cm) of the affinity membrane implied a poor dynamic binding efficiency, which can be explained by the intrinsic microstructures of the material. Although the electrospun membrane might not be an ideal candidate for the preparative affinity membrane chromatography for large-scale production, it still can be used for fast small-scale protein purification in which a highly efficient binding is not required. Spin columns packed with protein A/G immobilized PES membranes were demonstrated to be capable of binding IgG specifically. SDS-PAGE results demonstrated that the PES affinity membrane had high specific binding selectivity for IgG molecules and low non-specific protein adsorption. Compared with other reported affinity membranes, the PES affinity membrane had a comparable IgG binding capacity of 4.5 mg/ml, and had a lower flow through pressure drop due to its larger pore size. In conclusion, the novel PES affinity membrane is an ideal spin column packing material for fast protein purification.

© 2009 Elsevier B.V. All rights reserved.

1. Introduction

Electrospinning is a process utilizing high voltage electric field to produce polymer fibers of submicron or nano-scaled diameters from polymer solutions. Electrospun polymer fiber meshes have been extensively studied for various applications such as tissue engineering scaffolds [1] and gas or liquid filtration membranes [2,3]. They have also been functionalized with specific enzymes, for applications in membrane-based bioreactors [4–6].

Another major research interest for the electrospun polymer is as an affinity membrane [7–12]. Traditional affinity chromatography purification using gel bead-packed columns has certain limitations such as a high-pressure drop and low flow rate, while affinity membrane chromatography (AMC) provides an alternative solution [13,14]. By introducing capturing ligands into a membrane, selective capturing of target molecules from the filtrate can be

achieved. Due to the higher porosity and lack of diffusion resistance of affinity membranes, AMC has higher flow rates and lower pressure drop in comparison with the traditional column based chromatography, thus leading to improved throughput [15].

Previous work applying surface modified electrospun membranes as affinity membranes has been reported [7–12]. Electrospun chitosan nanofibers have been used for heavy metal ion removal from aqueous solution [11]. Surface functionalized electrospun Nylon nanofibers were applied for purification of papain [12]. In our previous work, cibacron blue (CB) has been immobilized on electrospun membranes to capture bovine serum albumin (BSA) [8,9]. Protein A/G immobilized electrospun cellulose membranes showed selective binding capacity for immunoglobulin G (IgG) [10]. However, these studies have not shown the dynamic binding efficiency of the electrospun affinity membranes in a quantitative way. In this work, dynamic binding efficiency of the electrospun affinity membranes was evaluated by frontal analysis. CB modified electrospun PES membranes were stacked into an AMC system and the breakthrough of the bovine serum albumin (BSA) solution through the AMC system was analyzed with the plate model. PES is a popular membrane material which is both physically and chemically strong and has intrinsic low non-specific protein binding properties. The

* Corresponding author at: McGowan Institute for Regenerative Medicine, University of Pittsburgh, 100 Technology Drive, Pittsburgh, PA 15219, United States. Tel.: +1 412 235 5166; fax: +1 412 235 5110.

E-mail address: maz@upmc.edu (Z. Ma).

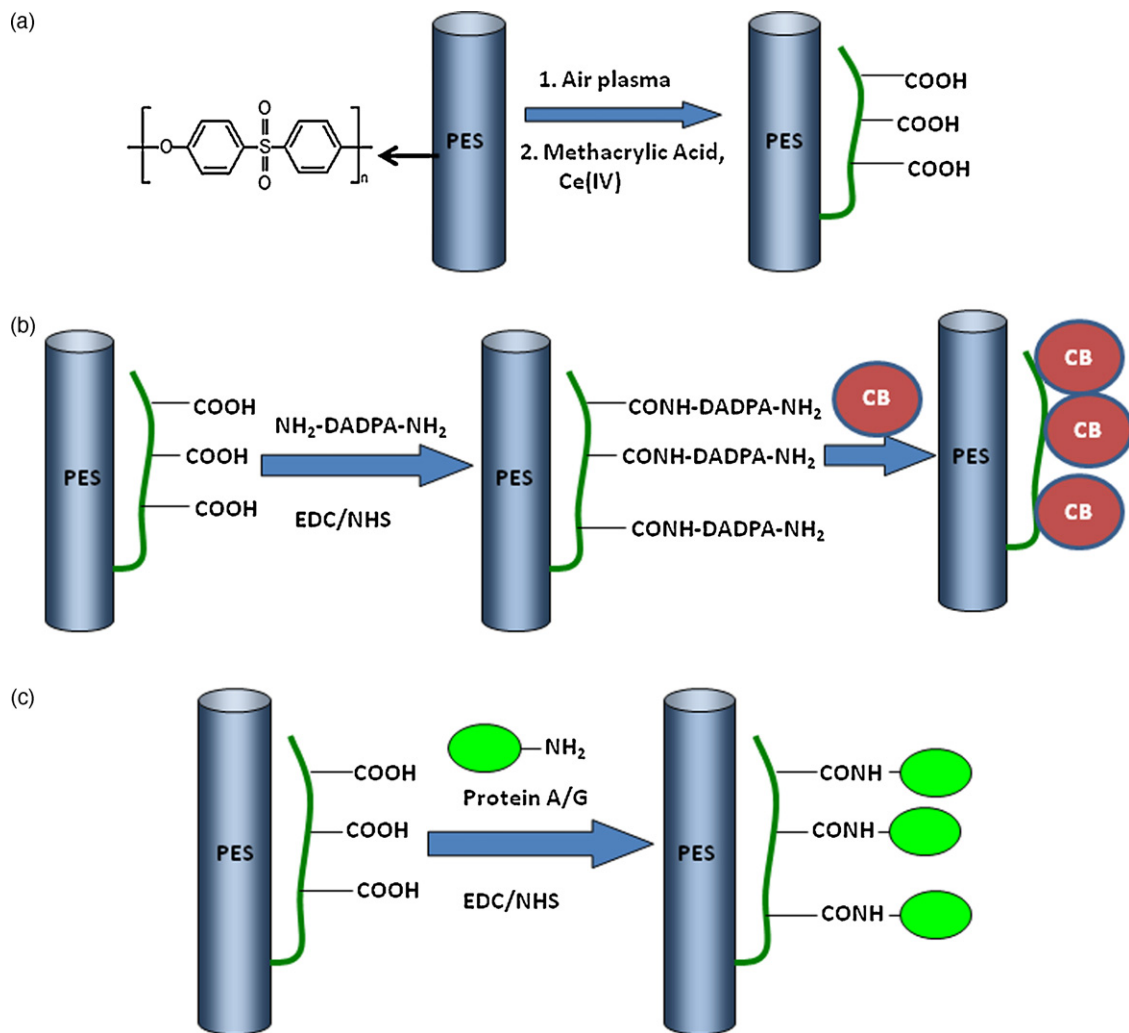


Fig. 1. Chemical reaction schemes for ligand immobilization on the membrane. (a) Graft polymerization of MAA; (b) immobilization of CB; (c) immobilization of protein A/G.

“CB-BSA” pair was chosen as a “ligand–absorbate” pair since it is popularly used as a research model for frontal analysis [16,17].

In addition to the dynamic binding efficiency study in which the electrospun PES affinity membranes were packed into an AMC system as a relatively large-scale protein production technique, the membranes were also studied as a packing material for spin column, a popular fast and small-scale protein purification tool in the laboratory. For this study, the ligand was chosen to be protein A/G which can specifically capture IgG. Protein A/G is a gene fusion product (Pierce) secreted from a non-pathogenic form of *Bacillus*, genetically engineered and combining the IgG binding profiles of both Protein A and Protein G. It has a molecular weight of 50,449 Daltons and contains 4 F_c binding domains from Protein A and 2 from Protein G. In this work, IgG purification performance of the spin columns packed with the protein A/G functionalized electrospun PES membranes was evaluated and the membrane was compared with other reported affinity membranes for IgG purifications.

2. Experiments

2.1. PES membrane preparation by electrospinning

PES granules (Goodfellow, M_w 55,000) were dissolved in DMF/Toulene (1:1, v/v) with a concentration of 0.25 g/ml. The solution was loaded into a 5-ml syringe and discharged by a syringe

pump at a speed of 3 ml/h. A 15-kV voltage was applied between the needle (27G) and aluminum plate (10 cm × 10 cm), with the distance between the needle tip and plate being 15 cm. A non-woven mesh of fibers was obtained on the aluminum plate, which was then heated at 245 °C for 1 h to improve its mechanical strength and structural integrity. The porosity of the membrane was evaluated using the equation, $\text{Porosity} = (1 - d/D) \times 100\%$, where D (1.37 g/cm^3) is the density of the material and d is the apparent density of the membrane obtained by dividing its mass by apparent volume (product of membrane area by thickness). The pore size of the PES membrane was determined by a capillary flow porometer (Porous Materials, Inc.) using bubble flow testing methods. Specific area of the membrane was measured with a BET nitrogen adsorption surface area analyzer (ASAP 2020 V3.00H, Micromeritics Co.).

2.2. Immobilization of CB on the PES membrane

CB was immobilized onto electrospun PES membranes using a method previously described in Ref. [8]. Briefly, poly(methacrylic acid) (PMAA) was grafted onto the membrane surface through Ce(IV) induced graft polymerization of methacrylic acid (MAA) with a graft polymerization time of 15 min [18] (Fig. 1a). The –COOH grafted PES membranes was determined with the Toluidine Blue O (TBO) method [19]. Diaminodipropylamine (DADPA) was then reacted with the PMAA grafted membrane with water-soluble carbodimide as the coupling agent to yield amino

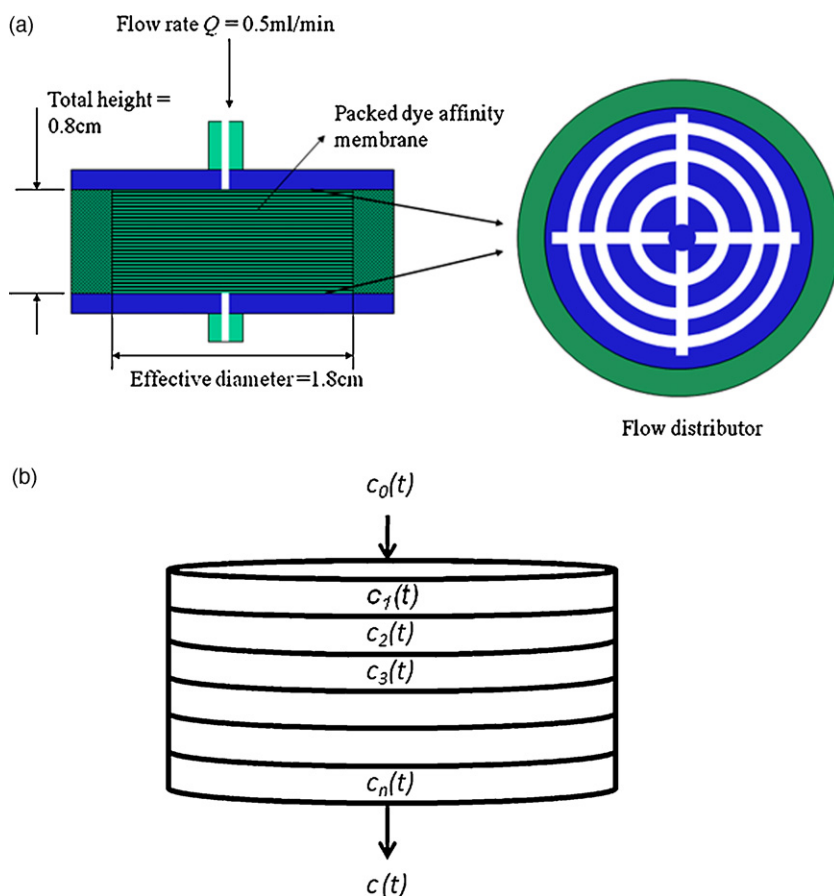


Fig. 2. Structure of the stainless steel membrane holder used for the BSA breakthrough curve analysis.

groups on the membrane surface [8]. Finally CB was reacted with the membrane to obtain the dye-functionalized affinity membrane, as shown in Fig. 1b. The CB density on the membrane was determined by measuring the mass increase of the membrane.

The adsorption isotherm of BSA on the CB immobilized affinity membrane was tested by immersing the affinity membrane in BSA solution in PBS (pH = 7.4) with different concentrations on a shaking bed for 24 h. The amount of the BSA adsorbed on the membrane was calculated by measuring the UV absorption at 280 nm of the BSA solution before and after the adsorption. The membranes were then regenerated by rinsing in PBS (pH = 10) containing 2 M NaCl for 3 h under stirring. The regenerated membrane showed the same adsorption curve as before. PES membranes grafted with PMAA and DADPA but without immobilization of the CB were used as a control. No adsorption of BSA on the control membranes was detected.

2.3. Breakthrough curve: experiments

The CB immobilized PES affinity membranes were cut into round shape with a diameter of 25 mm. Membranes (~160 layers, total height ~0.8 cm) were then stacked into a self-made stainless steel membrane holder as schematically shown in Fig. 2a. The dye affinity membranes packed in the filter holder has an effective diameter of 1.8 cm and therefore an effective area of 2.54 cm². The membrane holder was then mounted onto a liquid chromatography system (AKTATMFPLCTM, Amersham Pharmacia Biotech). After rinsing the dye affinity membrane with PBS (pH = 7.4), BSA solution in PBS (pH = 7.4) with a concentration of 0.2 mg/ml was injected into the membrane holder with injection speeds of 0.2, 0.5 or 1 ml/min. Breakthrough curves were obtained by continuously monitoring the concentration of the eluted BSA solution with a UV detector at

280 nm. PES membranes grafted with PMAA and DADPA but without CB were used as a control to obtain non-adsorption curves. The dead volume of the filter holder, 0.8 ml, was subtracted from the elution volume (V_e) of all the experimental breakthrough curves.

2.4. Breakthrough curve: simulation

Simulation of the breakthrough curve of the AMC process was conducted using the plate model [20], in which the column is assumed to be divided into discrete plates and in every plate the solute concentration in mobile phase (c) and in stationary phase (c_s) are assumed to be in instantaneous equilibrium. Linear adsorption relation $c_s = Kc$ applies when the feeding concentration of the solute is small, where K is the distribution coefficient. As shown in Fig. 2b, the column plate number n is $n = L/H_p$ where L is the total height of the membrane stack and H_p is the plate height. Let $c_0(t)$, $c_1(t)$, $c_2(t)$, $c_3(t)$... $c_n(t)$ represent the feeding concentration and concentration of the mobile phase in the 1st, 2nd, 3rd... n th plate, respectively. Mass conservation equation for the first plate gives:

$$\frac{dc_1(t)}{dt} + Ac_1(t) = Ac_0(t) \quad (\text{the 1st plate}) \quad (1)$$

in which $A = Q/(V_p \varepsilon (K' + 1))$, where ε is the porosity of the stationary phase, $V_p = \pi r^2 H_p$ is plate volume, K' is $((1 - \varepsilon)/\varepsilon)/K$ and Q is the volume flow rate of the mobile phase. Similarly, for the 2nd, 3rd... n th plate the following equation applies:

$$\frac{dc_2(t)}{dt} + Ac_2(t) = Ac_1(t) \quad (\text{For the 2nd plate}) \quad (2)$$

$$\frac{dc_n(t)}{dt} + Ac_n(t) = Ac_{n-1}(t) \quad (\text{For the } n\text{th plate}) \quad (3)$$

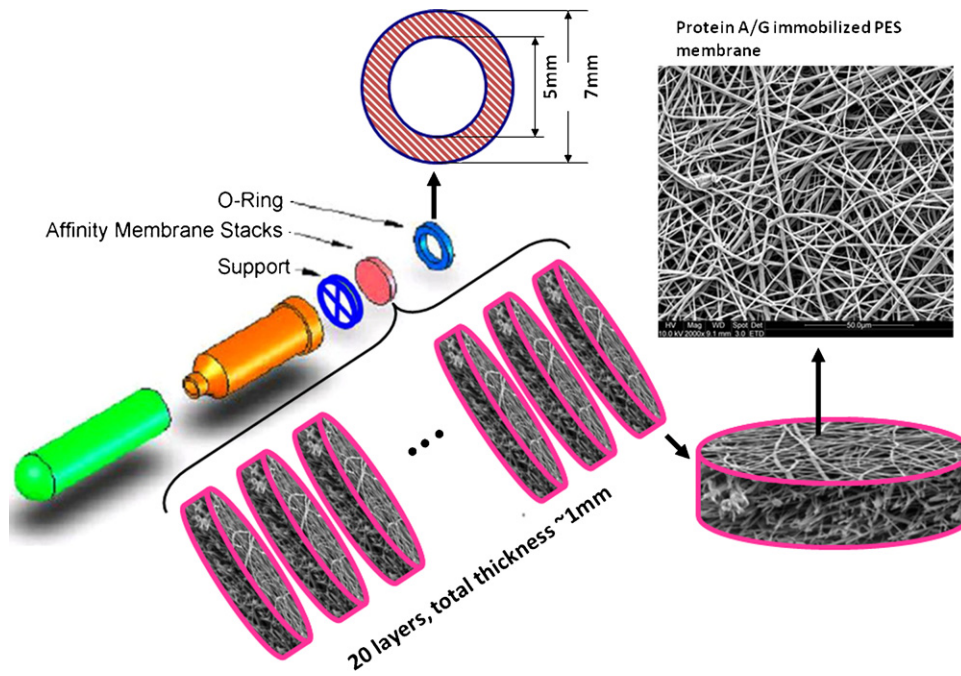


Fig. 3. Structure of the spin column. The SEM image on the upper right corner shows the protein A/G functionalized membrane.

Eqs. (1)–(3) compose a differential equation system consisting of n linear differential equations with n functions, $c_1(t)$, $c_2(t)$, $c_3(t)$... $c_n(t)$ to be solved, with a given $c_0(t)$ and the initial conditions, $c_1(0) = c_2(0) = c_3(0) \dots = c_n(0) = 0$. It was demonstrated [21] that application of the Laplace transform leads to solving of the $c_n(t)$ easily with the solution as

$$c_n(t) = \left\{ A^n \frac{t^{n-1}}{(n-1)!} e^{-At} \right\} \otimes \{c_0(t)\} \\ = \int_0^t A^n \frac{(t-\lambda)^{n-1}}{(n-1)!} e^{-A(t-\lambda)} c_0(\lambda) d\lambda \quad (4)$$

This allows simulation of a breakthrough curve with any feeding function $c_0(t)$. When $c_0(t)$ is a time-independent constant c_0 , Eq. (4) becomes:

$$\frac{c(t)}{c_0} = \int_0^t A^n \frac{(t-\lambda)^{n-1}}{(n-1)!} e^{-A(t-\lambda)} d\lambda \quad (5)$$

The $c_n(t)$ is simplified as $c(t)$ in Eq. (5). The function $c(t)/c_0$ can also be expressed as a function of elution volume (V_e) based on the relationship $V_e = Qt$. Eq. (5), however, can only be applied when the plate number n is an integer, otherwise the factorial $(n-1)!$ in the equation will be meaningless. This problem can be solved by replacing the factorial $(n-1)!$ with the Gamma function $\Gamma(n)$ [22], therefore:

$$\frac{c(t)}{c_0} = \int_0^t A^n \frac{(t-\lambda)^{n-1}}{\Gamma(n)} e^{-A(t-\lambda)} d\lambda \quad (6)$$

Eq. (6) applies even when n is not an integer or is smaller than one.

2.5. Immobilization of protein A/G on the PES membrane and spin column packing

First, poly(methacrylic acid) (PMAA) was grafted onto the PES membrane as described above. The PMAA grafted membranes were cut into circular pieces of 7 mm diameter after which a stack of 20 membranes (thickness, 1 mm) were packed into the spin column. An O-ring was pressed on top of the membrane stacks, supported

firmly by an inert support below, to hold the membranes in place (Fig. 3). The active filtration area was 19.6 mm^2 .

The carboxyl ($-\text{COOH}$) groups on the PMAA grafted PES nanofiber membranes were activated before reacting with protein A/G. At 4°C , 1-ethyl-3-(3-(dimethylamino)propyl)carbodiimide hydrochloride (EDC, 100 mg/ml) and *N*-hydroxyl succinimide (NHS, 100 mg/ml) mixture solution in 2-(*N*-morpholino)ethanesulfonic acid (MES, 0.1 M, pH 5.0) was added into the spin column and the solution was allowed to flow through the PMAA membranes by gravity for 4 h at a flow rate of 1 ml/h. The membrane was then rinsed off with PBS three times by centrifuging (500 rpm, Eppendorf Centrifuge 5417C). Finally, protein A/G solution (5 mg/ml in PBS) was repeatedly flowed through the spin column for 24 h at 4°C . After that, the membranes were rinsed with 1% Tween 20 solution and then with PBS three times by centrifuging to remove free protein A/G. Bicinchoninic acid (BCA) protein assay kit (Pierce) was used for the determination of the protein A/G density on the membrane.

To obtain the adsorption isotherm of IgG on the protein A/G immobilized membrane, solutions of IgG in Pierce ImmunoPure® (A/G) IgG Binding Buffer/PBS (1:1, v/v) with different concentrations were filtered through the spin column at room temperature and then the membranes were immersed in the IgG solution for 24 h under shaking to reach equilibrium. Then, the IgG captured by the membranes was eluted, and the amounts of the eluted IgG were determined by UV (280 nm), and were plotted against the IgG concentration at equilibrium. In this work PMAA grafted PES membranes without further immobilization of protein A/G were used as the non-adsorption control membranes. No non-specific adsorption of either IgG or BSA was found on the control membranes, because the PMAA grafted membrane is highly hydrophilic.

2.6. Efficiency test of the protein A/G functionalized spin column

The IgG solution to be purified consists of 1.12 mg/ml Human IgG (Technical Grade, Sigma) and $400 \mu\text{g/ml}$ BSA dissolved in Pierce ImmunoPure® (A/G) IgG Binding Buffer/PBS (1:1, v/v), where the BSA was used as a model impurity. First, the spin column was pre-washed with the Pierce ImmunoPure® (A/G) IgG Binding Buffer/PBS

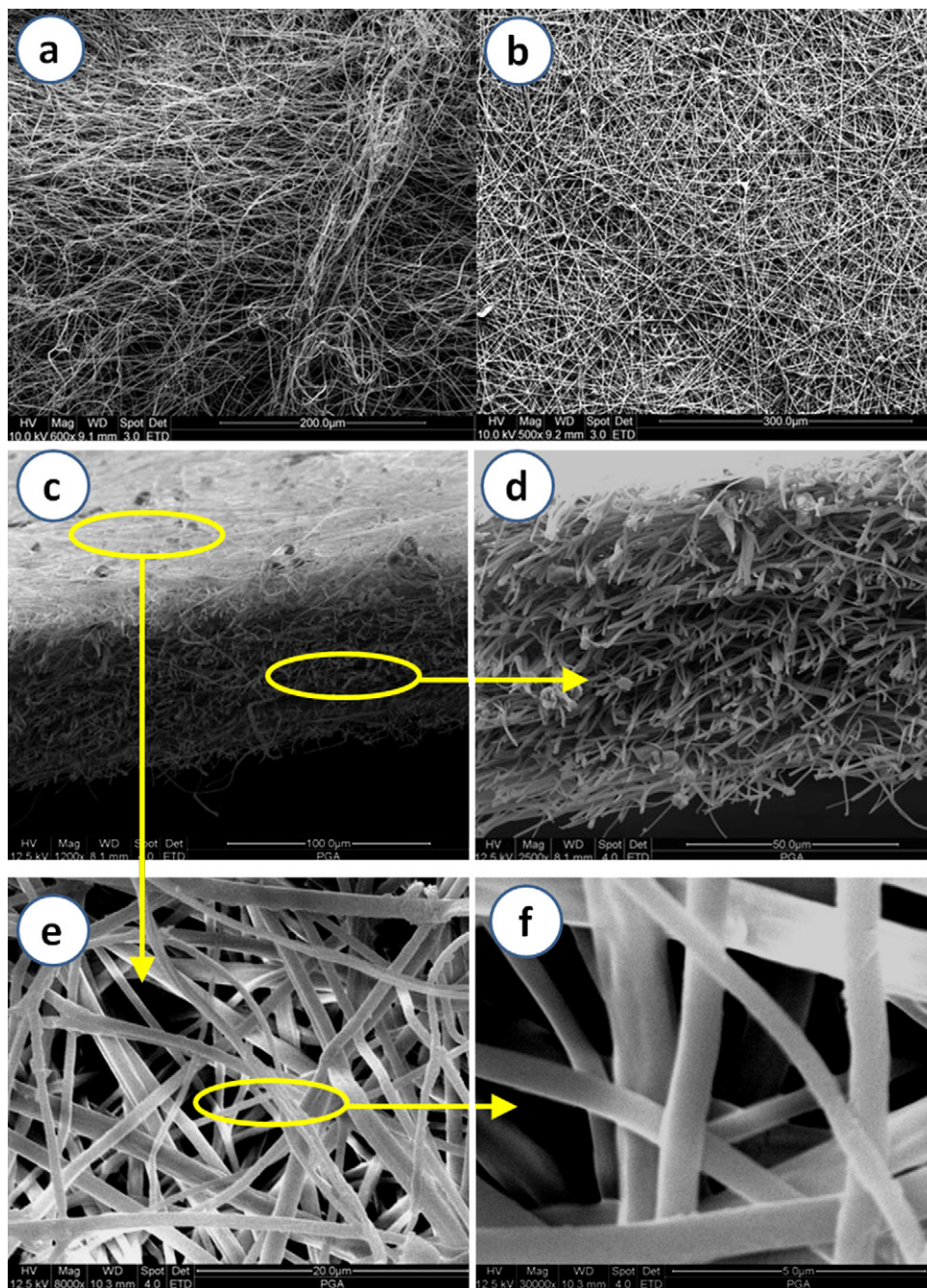


Fig. 4. SEM images showing the electrospun PES membrane's microstructure: (a) untreated membrane; (b–f) heat-treated membrane; (c) surface and cross-section; (d–f) magnified images of the membrane's cross-section and surface morphology.

(1:1, v/v) twice. The IgG/BSA sample solution (300 μ l) was filtered through the spin column at a centrifuge speed of 500 rpm ($26.5 \times g$). The sample were then collected and filtered again. Because it takes the sample 1 min to pass through the entire column at 500 rpm, this process was repeated a total of 6 times to simulate a 6-min standing time of the sample in the column. The column was then washed twice with 500 μ l Pierce ImmunoPure[®] (A/G) IgG Binding Buffer/PBS (1:1, v/v) to remove free proteins in the column, followed by washing twice with 500 μ l of PBS. This second PBS washing is necessary because any remaining basic (pH 8.2) binding buffer solution would affect the acidic elution buffer's function. Finally 300 μ l of elution buffer (Pierce ImmunoPure[®] IgG) was run through the column 6 times at a centrifugal speed of 500 rpm. The eluted solution is evaluated by SDS-PAGE analysis performed on

a Mini-PROTEAN[®] 3 Cell System (BIORAD), with 4% stacking and 12% resolving gel formula adopted. SDS-PAGE Molecular Weight Standards Kit Broad Range (BIORAD) was used for calibration.

3. Results and discussion

3.1. Membrane preparation

A non-woven mesh of PES fibers with submicron scaled diameter were obtained by electrospinning. Heat treatment allowed the fibers to adhere to one another to improve the mechanical strength and structural integrity of the mesh [23]. Without heat treatment, handling of the mesh would be difficult since it is a cotton-like fluffy

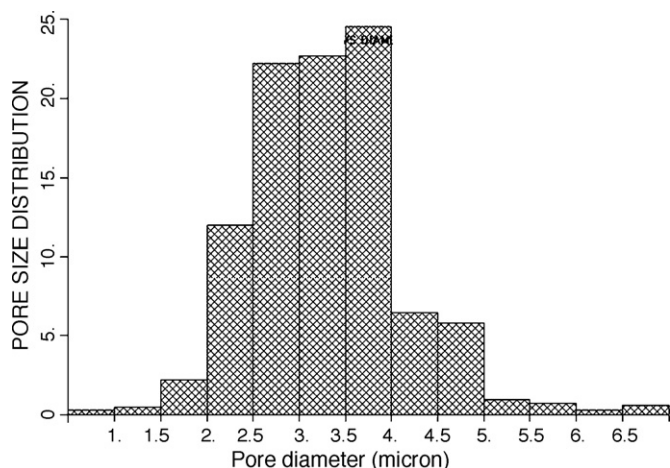


Fig. 5. Histogram of the pore size distribution of the electrospun PES membrane.

and sticky material. Heat treatment has to be done at a temperature between the glass transition temperature (220 °C) and melting temperature (345–390 °C) of the PES to allow fusion of the fibers while still maintaining its fibrous morphology. The temperature of 245 °C was found to be suitable. Fig. 4 shows the SEM pictures of the membrane before and after heat treatment (245 °C for 1 h). While the untreated membrane easily lost its structure under external mechanical force (as shown in Fig. 4a), the heat-treated membrane was much more steady (Fig. 4b).

Fig. 4c–d shows detailed microstructures of the heat-treated PES membrane. The fiber diameter ranged from 450 nm to 2.0 μm as found from the SEM observation. The electrospun membrane is highly porous, with an apparent density of 0.394 g/cm³. Since the bulk density of PES is 1.37 g/cm³, the porosity of the PES membrane can be calculated to be 71%. Using bubble point tests, the mean flow pore size of the membrane was determined as 3.3 μm and the bubble point pore diameter was 6.8 μm. Pore size distribution of the membrane is shown in Fig. 5. Specific surface area of the membrane was determined as 4 m²/g using a BET nitrogen adsorption surface area analyzer.

3.2. Ligand immobilization

The chemical inertness of PES raises a challenge for chemical surface modification of the membrane. A previously developed surface graft polymerization technique [18] to yield –COOH groups on chemically inert polymer surface was utilized in this work. The PES nanofiber membrane was first treated by air plasma, followed by cerium (IV) ion induced radical polymer graft polymerization of MAA (Fig. 1a). Successful graft polymerization of MAA was verified by directly checking the existence and quantifying the amount of the carboxyl groups (–COOH) on the membrane. A density of 47 nmol/mg –COOH groups on the membrane was found to be present. Two kinds of ligands, CB or protein A/G, were immobilized onto the PMAA grafted PES membrane, as shown in Fig. 1b and c. For the CB immobilized membrane, a CB density of 25 mg/g (9.9 mg/ml) was measured, while for the Protein A/G immobilized membrane, a protein A/G density of 7.5 μg/mg (3.0 mg/ml) was determined.

3.3. Dynamic binding efficiency of BSA on the CB functionalized membrane

The adsorption isotherm of BSA on the CB modified membrane is shown in Fig. 6. No adsorption of BSA on the control membranes (with CB) was observed, which may be attributed to the strong hydrophilicity of DADPA on the membrane surfaces. Thus

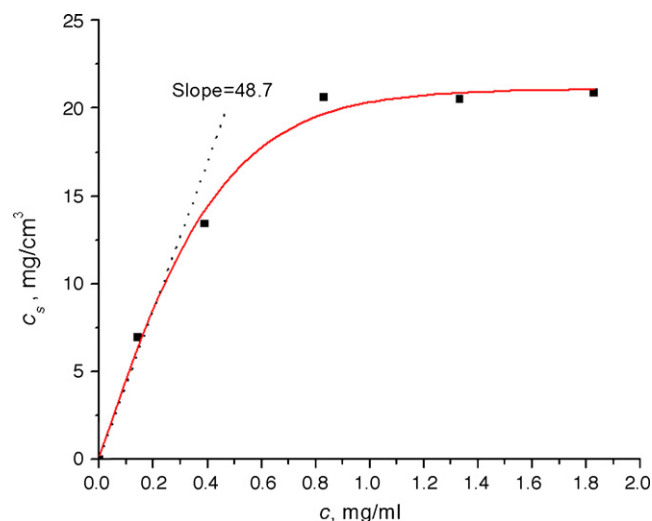


Fig. 6. BSA adsorption curve on the CB functionalized membrane.

the adsorption of BSA on the dye affinity membrane can be mainly attributed to the specific interactions between the CB and the BSA molecules. Fig. 6 shows that when the concentration of the BSA solution is smaller than 0.2 mg/ml, the adsorption curve is approximately linear with a slope of $K=48.7$. Therefore, in the frontal analysis experiment, the fed BSA concentration is chosen at 0.2 mg/ml to satisfy a linear adsorption. Fig. 7 shows the experimental breakthrough curves of the BSA solution and the theoretical breakthrough curves corresponding to different H_p values calculated based on Eq. (6). Comparing between the experimental curves and the theoretical curves will allow the H_p of the affinity membrane to be evaluated.

First, theoretical breakthrough curves corresponding to different H_p values were calculated according to Eq. (6) as follows. Since $K=48.7$ and the membrane's porosity ε (71%) was known, $K'=((1-\varepsilon)/\varepsilon)K$ was known. Since the packed affinity membranes had a total height of $L=0.8$ cm and an effective radius of $r=0.9$ cm (see Fig. 2a), if H_p is known, the plate number (n) will be known as $n=L/H_p$ and the plate volume (V_p) will be known as $V_p=\pi r^2 H_p$. At a given Q , $A=Q/V_p \varepsilon (K'+1)$ can be calculated and finally the breakthrough curves can be calculated by Eq. (6). For $Q=0.5$ ml/min, the theoretical breakthrough curves corresponding to $H_p=0.04$ cm ($n=20$; $A=0.332$ min⁻¹), $H_p=0.08$ cm ($n=10$; $A=0.166$ min⁻¹), $H_p=0.16$ cm ($n=5$; $A=0.083$ min⁻¹), $H_p=0.8$ cm ($n=1$; $A=0.0166$ min⁻¹), $H_p=1.6$ cm ($n=0.5$; $A=0.0083$ min⁻¹), $H_p=4$ cm ($n=0.2$; $A=0.00332$ min⁻¹) and $H_p=8$ cm ($n=0.1$; $A=0.00166$ min⁻¹) are shown in Fig. 7a. It can be seen that the binding efficiency increases with plate number (n). Higher plate numbers will give a much sharper breakthrough than lower plate numbers. A high plate number (or small H_p) corresponds to an ideal situation in which breakthrough would occur only after the binding of the protein by the ligand reaches saturation, at which point the effluent concentration would instantaneously increase from zero to that of the feed solution [24,25]. On the other hand, actual breakthrough curves are often broadened by the non-idealities of real flow systems, e.g., dead volume mixing and flow maldistribution, and by slow intrinsic sorption kinetics [24]. The non-ideal breakthrough corresponds to the situations when the n is low (or H_p is large). As shown in Fig. 7a, the breakthrough curves corresponding to smaller plate numbers (such as $n \leq 1$) are very broad. In these cases the breakthrough occurs at the very beginning of the elution, followed by a slow and gradual increase in the concentration of the effluent, which indicates a poor dynamic binding efficiency [24,25].

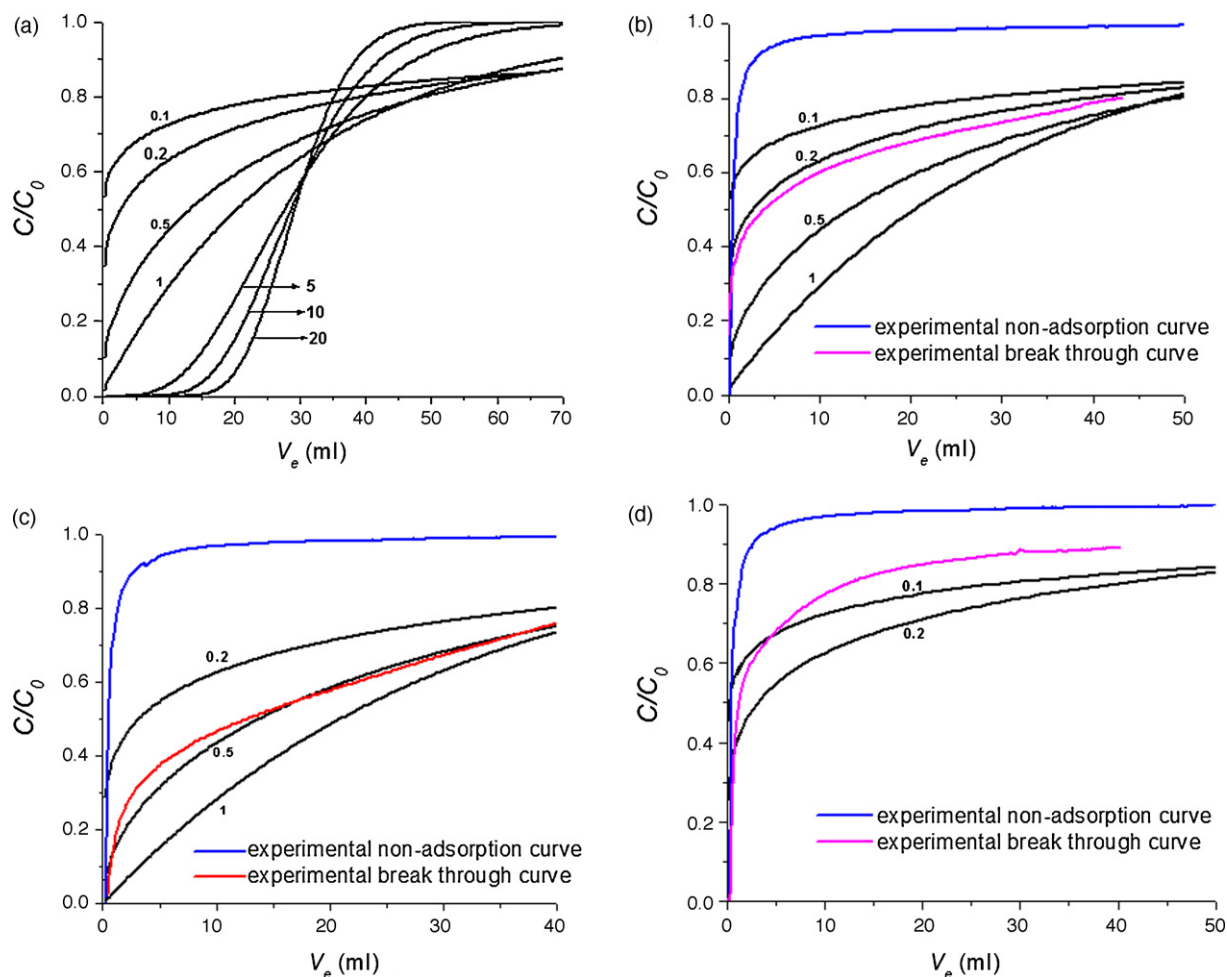


Fig. 7. Theoretical and experimental breakthrough curves of BSA solution through the stacked PES affinity membranes at flow rate of (a and b) 0.5 ml/min, (c) 0.2 ml/min and (d) 1 ml/min. The numbers in the figures are assumed plate numbers for calculation of the corresponding theoretical curves. The non-adsorption curve was obtained using hydrophilic control PES membranes without CB immobilization.

Fig. 7b shows the experimental breakthrough curve of the PES affinity membrane system at a flow speed of $Q=0.5$ ml/min. An experimental non-adsorption curve obtained with control membranes without CB is also shown. The broadened breakthrough curve of the affinity membrane typically reflects a poor binding efficiency. Compared with the much sharper breakthrough curves of other affinity membranes [16,17] with CB-BSA as a ligand–ligate pair, it can be concluded that the electrospun PES affinity membrane's binding efficiency is poor. In Fig. 7b, by comparing the experimental breakthrough curve with the theoretical curves corresponding to different plate number (n) or plate height (H_p), the affinity membrane's H_p can be estimated as ~ 4 cm ($n=0.2$). Using the same process, the H_p of the affinity membrane at flow speed of 0.2 and 1 ml/min was evaluated as ~ 1.6 cm and >8 cm, respectively, as shown in Fig. 7c and d. The affinity membrane's H_p is inversely affected by the flow speed due to the fact that a slower speed will allow enough time for the BSA molecules to be captured.

The reason for the low binding efficiency of the PES affinity membrane can be attributed to several factors. First and most important, the PES membrane has a high porosity of 71%, therefore the BSA molecules in the mobile phase in the interstitial space of the membrane may not have enough chance to interact with the fiber surfaces. The second reason may be the membrane's relatively small specific surface area ($4\text{ m}^2/\text{g}$). Commercialized traditional column packing materials like silica gel or hydrogel beads usually have specific surface area of $200\text{--}800\text{ m}^2/\text{g}$ [26]. The low surface

area of the membrane decreases the chance for the BSA molecules to be captured. Third, a broad flow rate distribution in the membrane may be caused by the wide pore size distribution (Fig. 5) and the intrinsic non-woven fibrous feature. Therefore, to improve the membrane's dynamic binding efficiency, future efforts need to be focused on decreasing the porosity and increasing the specific surface area of the membrane. A smaller diameter would be desirable since this will lead to higher specific surface area.

3.4. Protein A/G immobilized membrane

The low dynamic binding efficiency of the electrospun PES affinity membrane demonstrated that the material might not be an ideal candidate for the preparative AMC process for large-scale protein production. However, it is still possibly usable for fast small-scale protein purification in which a high recovery rate is often not necessary. To demonstrate this, the electrospun PES membranes were functionalized with protein A/G (Fig. 1c) aiming at IgG purification.

Binding capacity of the membrane for IgG was studied, as shown in Fig. 8. Using a least square fitting method, the experimental adsorption isotherm was fitted with the Langmuir adsorption model, $q = q^*c/(K_d + c)$, where q is the adsorption density (expressed as mass of IgG adsorbed on unit mass of membrane), q^* is the capturing capacity (saturated adsorption density), c is the IgG solution concentration and K_d is the dissociation constant of the ligand–ligate complex. Fitting the experimental data with the Lang-

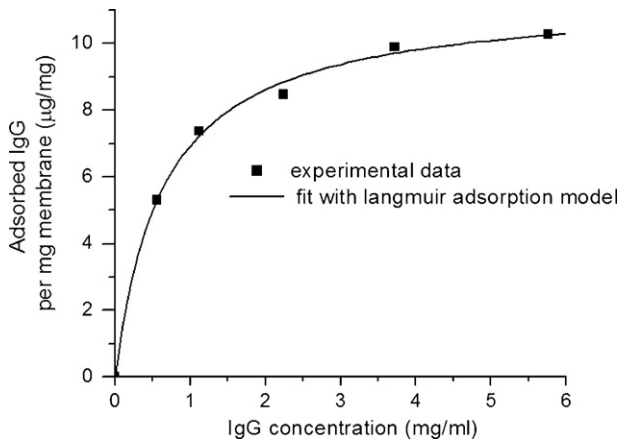


Fig. 8. Adsorption curve of IgG on the protein A/G immobilized PES affinity membranes.

muir adsorption model gave a capturing capacity (q^*) of 11.4 $\mu\text{g}/\text{mg}$ (4.5 mg/ml) and a dissociation constant (K_d) of 0.6476 mg/ml.

Knowing the molecular weight of protein A/G and IgG (50 K and 146 K, respectively), the protein A/G density (7.5 $\mu\text{g}/\text{mg}$ or 3.0 mg/ml) and the IgG binding capacity (11.4 $\mu\text{g}/\text{mg}$ or 4.5 mg/ml), the molar ratio of the protein A/G to the IgG can be calculated as 2:1. Considering that every Protein A/G molecule has 6 IgG binding sites, it can be concluded that only 1/12 of the binding domains were effectively utilized for IgG binding. To improve the IgG binding capacity, obviously a higher ligand (Protein A/G) density is desired. This can be realized by decreasing the fiber diameter of the membrane since the specific area should be reversely proportional to the square of the fiber diameter. The current membrane has fiber diameter range of 0.45–2 μm and a specific area of 4 m^2/g . Therefore, decreasing the fiber diameter to 0.2–1 μm would allow the specific area to be increased by 4 times, i.e. 16 m^2/g .

To test the IgG purification efficiency of the protein A/G functionalized affinity membrane, spin columns packed with the affinity membrane were prepared and used for IgG purification. BSA (400 $\mu\text{g}/\text{ml}$) was added into the IgG solution (1120 $\mu\text{g}/\text{ml}$) as a model impurity and the IgG was purified from the mixture with the spin column and was then analyzed with SDS-PAGE. Since SDS-PAGE was run under denaturing conditions, one IgG molecule was decomposed into two heavy chains (50 K) and two light chains (25 K), leading to two bands corresponding to IgG, as shown in Fig. 9. The impurity (BSA) band was not present after the purification process, as shown in band 3 in Fig. 9. No protein bands were observed for the control membrane packed spin column. These results indicated the affinity membrane had specific binding for IgG and low non-specific protein binding. Reusability of the PES affinity membrane was also demonstrated. There was no degradation of the membrane's binding ability in the process of purifying 10 samples over a 3-month period. Fig. 9 also shows the band corresponding to the purified IgG from the spin column at its 10th time of use.

3.5. Comparison with other affinity membranes

It is interesting to compare the performance of the PES affinity membrane with other affinity membranes for IgG purification. As described above, the IgG binding capability of the PES affinity membrane was measured as 11.4 $\mu\text{g}/\text{mg}$ (4.5 mg/ml). This is comparable with reported IgG binding capacities of other affinity membranes [25,27]. A protein A functionalized poly(methyl methacrylate, acrylonitrile and sodium methallyl sulfonate) membrane (Tech-sep, Miribel, France) with a porosity of 70% and pore size of 0.6–1 μm was shown to have an IgG binding capacity of 6.6 mg/ml [25]. Another protein G functionalized cellulose affinity membrane (MemSep 1000, Millipore Corp., Bedford, MA) with pore size of 1.2 μm and porosity of 85% was reported to have an IgG binding capacity of 5.8 mg/ml [27]. The smaller pore sizes of these membranes compared with that of the PES membrane (3–4 μm) in

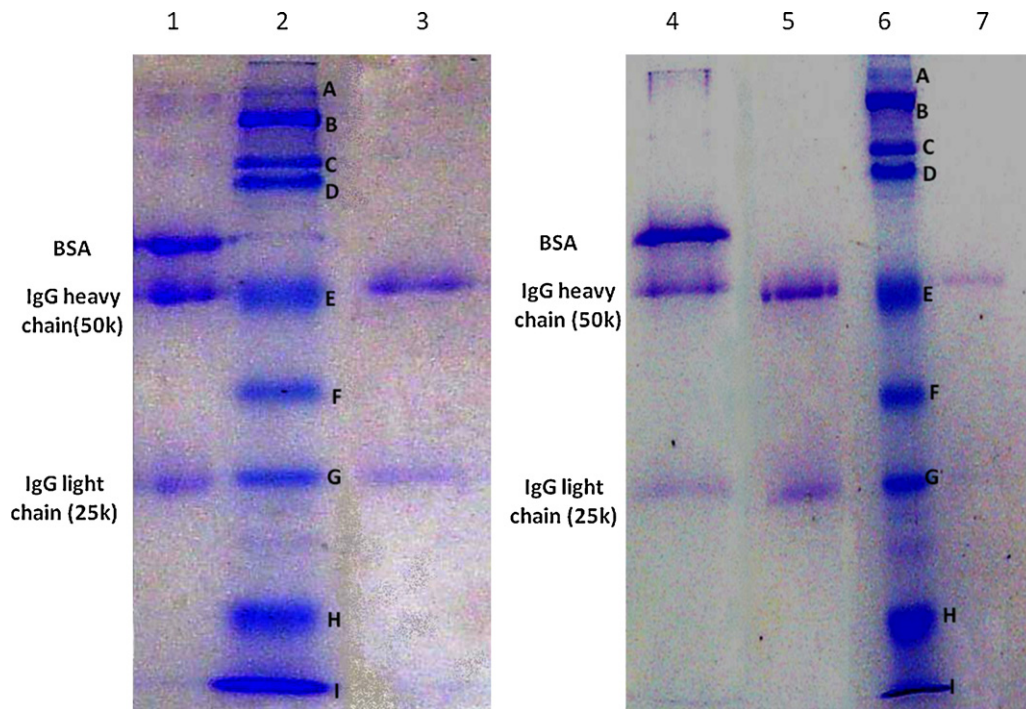


Fig. 9. SDS-PAGE results of the IgG samples purified by a spin column packed with the PES affinity membrane for its 1st time use (band 3 in a) and its 10th time use (band 5 in b). Specifically, 1: IgG containing BSA as impurities; 2: standards; 3: purified IgG; 4: IgG containing BSA as impurities; 5: purified IgG; 6: standards; 7: IgG purified with spin column packed with commercial affinity membrane. Proteins standards: (A) myosin 200,000; (B) β -galactosidase 116,250; (C) phosphorylase b 97,400; (D) serum albumin 66,200; (E) ovalbumin 45,000; (F) carbonic anhydrase 31,000; (G) trypsin inhibitor 21,500; (H) lysozyme 14,400; (I) aprotinin 6500.

this work might be the reason of their higher IgG binding capacity since smaller pore size might cause higher specific area. A commercial affinity membrane (Sartobind® Protein A 75 Membrane Adsorbers, pore size 0.45 μm) functionalized with recombinant Protein A has a claimed IgG binding capacity of 80 $\mu\text{g}/\text{cm}^2$. Since the average area density of this membrane was measured to be 8.6 mg/cm^2 , its IgG binding capacity was calculated as 9.3 $\mu\text{g}/\text{mg}$, which is close to the binding capacity (11.4 $\mu\text{g}/\text{mg}$) of the PES affinity membrane in this work.

Compared with those membranes described above, the PES affinity membrane has an advantage of easier filtrate flow through due to its larger pore size (3–4 μm , see Fig. 5). To demonstrate this, a Sartobind® ProteinA75 Membrane Adsorbers unit was disassembled and the membranes were packed into a spin column (8 layers, ~ 1 mm). The centrifuge speed required for 300 μl of PBS to flow through spin columns packed with the PES affinity membranes or the commercial membranes in 1 min was determined. To do so, spin columns containing 300 μl PBS were centrifuged for 1 min at different rotation speeds. While a centrifuge speed of only 500 rpm (26.5 $\times g$) is needed for the PES membrane packed columns, the commercial affinity membrane packed columns need a centrifuge speed of 2000 rpm (424.5 $\times g$) to achieve a comparable flow rate. Fig. 9 also showed the SDS-PAGE result of the IgG purified by the commercial membrane packed spin column. Although the IgG was highly purified (BSA disappeared), the IgG bands were fainter than that purified by the PES membrane packed spin column. It is possible that leakage through the side of the commercial membrane packed spin columns is much more likely than for the PES membrane packed spin columns, given the higher centrifuge speed needed for the commercial membrane. However, this by no means implies a worse performance of the commercial membrane. In fact, the membranes are originally packed into a tightly sealed syringe filter by the manufacturer and they are intended to be used by pressing the sample through the membranes with a syringe with a luer lock connector, in which the possibility of leakage is excluded.

4. Conclusions

Frontal analysis of the electrospun affinity membrane with CB-BSA as a model ligand–ligate pair demonstrated that the mem-

brane has poor dynamic binding efficiency, which can be attributed to the material's intrinsic microstructure properties such as high porosity and low specific surface area. Although the electrospun PES membrane might not be an ideal candidate for preparative AMC processes for large-scale production, it was shown to be a potentially ideal candidate as a fast protein purification tool on a small-scale basis. Protein A/G immobilized membrane with a density of 7.5 $\mu\text{g}/\text{mg}$ (3.0 mg/ml) showed an IgG binding capacity of 11.4 $\mu\text{g}/\text{mg}$ (4.5 mg/ml) which is comparable with a commercial product. Spin columns packed with the affinity membrane showed high specific binding for IgG, good reusability and low filtration pressure drop.

References

- [1] Z.W. Ma, M. Kotaki, R. Inai, S. Ramakrishna, *Tissue Eng.* 11 (2005) 101.
- [2] P. Gibson, H. Schreuder-Gibson, D. Rivin, *Colloids Surf. A. Physicochem. Eng. Asp.* 187 (2001) 469.
- [3] R. Gopal, S. Kaur, Z.W. Ma, C. Chan, S. Ramakrishna, T. Matsuura, *J. Membr. Sci.* 281 (2006) 581.
- [4] S. Sakai, K. Antoku, T. Yamaguchi, K. Kawakami, *J. Membr. Sci.* 325 (2008) 454.
- [5] Y. Wang, Y.L. Hsieh, *J. Membr. Sci.* 309 (2008) 73.
- [6] L. Wu, X. Yuan, J. Sheng, *J. Membr. Sci.* 250 (2005) 167.
- [7] Z.W. Ma, K. Masaya, S. Ramakrishna, *J. Membr. Sci.* 272 (2006) 179.
- [8] Z.W. Ma, K. Masaya, S. Ramakrishna, *J. Membr. Sci.* 282 (2006) 237.
- [9] Z.W. Ma, M. Kotaki, S. Ramakrishna, *J. Membr. Sci.* 265 (2005) 115.
- [10] Z.W. Ma, S. Ramakrishna, *J. Membr. Sci.* 319 (2008) 23.
- [11] S. Haider, S.Y. Park, *J. Membr. Sci.* 328 (2009) 90.
- [12] H. Zhang, H. Nie, S. Li, Y. Xue, L. Zhu, *J. Biotechnol.* 136 (2008) S416.
- [13] E. Klein, *J. Membr. Sci.* 179 (2000) 1.
- [14] H. Zou, Q. Luo, *J. Biochem. Biophys. Methods* 49 (2001) 199.
- [15] J. Tomas, M.R. Kula, *Biotechnol. Prog.* 11 (1995) 357.
- [16] W. Hao, J. Wang, J. Li, *Chromatographia* 60 (2004) 449.
- [17] W. Hao, J. Wang, *J. Chromatogr. A* 1063 (2005) 47.
- [18] Z.W. Ma, S. Ramakrishna, *J. Appl. Polym. Sci.* 101 (2006) 3835.
- [19] E. Uchida, Y. Uyama, Y. Ikada, *Langmuir* 9 (1993) 1121.
- [20] J. Cases, R.P.W. Scott, *Chromatography Theory*, Marcel Dekker, Inc., New York, 2002, p. 261.
- [21] V. Deemter, *Chem. Eng. Sci.* 5 (1956) 271.
- [22] A. Velayudhan, M.R. Ladisch, *Adv. Biochem. Eng. Biot.* 49 (1993) 123.
- [23] H.Y. Chung, US Patent 6,743,273, June 1, 2004.
- [24] S.Y. Suen, M.R. Etzel, *Chem. Eng. Sci.* 47 (1992) 1355.
- [25] O.P. Dancette, J.L. Taboureau, E. Tournier, C. Charcosset, P. Blond, *J. Chromatogr. B* 723 (1999) 61.
- [26] H. Izutsu, F. Mizukami, P.K. Nair, Y. Kiyozumi, K. Maeda, *J. Mater. Chem.* 7 (1997) 767.
- [27] J.E. Kochan, Y.J. Wu, M.R. Etzel, *Ind. Eng. Chem. Res.* 35 (1996) 1150.